Kinetics and Catalysis, Vol. 45, No. 4, 2004, pp. 589–597. Translated from Kinetika i Kataliz, Vol. 45, No. 4, 2004, pp. 622–631.

CATALYTIC REACTION MECHANISMS

Selective Catalytic Oxidation of Methane to Syngas over Supported Mixed Oxides Containing Ni and Pt

S. N. Pavlova, N. N. Sazonova, V. A. Sadykov, O. I. Snegurenko, V. A. Rogov, E. M. Moroz, I. A. Zolotarskii, A. V. Simakov, and V. N. Parmon

Boreskov Institute of Catalysis, Siberian Division, Russian Academy of Sciences, Novosibirsk, 630090 Russia

Received February 14, 2003

Abstract—The activity of Ni, Pt, and $LaNiO_3$ supported on α-Al_2O_3 is studied in the selective catalytic oxidation of methane to syngas at 900°C and a contact time of ~0.002 s using dilute mixtures (1000 ppm CH_4 + 500 ppm O_2 in He). The grain size was ~100 μm. The method of X-ray phase analysis shows that supported $LaNiO_3$, both pure and containing Pt, has a perovskite hexagonal structure with altered lattice parameters. Using temperature-programmed reduction by hydrogen, it was found that the reduction of supported $LaNiO_3$ is simplified in the presence of Pt and/or $Ce_{0.2}Zr_{0.8}O_2$. The activity and selectivity of the catalysts in the reaction of selective catalytic oxidation of methane depends on their composition and oxidative–reductive treatment. It was found that, in the presence of catalysts based on $LaNiO_3$ and containing Pt and/or $Ce_{0.2}Zr_{0.8}O_2$, the reaction occurs with an induction period. It was assumed that the value of the induction period depends both on the dynamics of phase $LaNiO_3$ reduction to Ni, which is associated with the accumulation of carbonate complexes and surface hydroxylation, and on slow changes in the defect structure of $Ce_{0.2}Zr_{0.8}O_2$, which are associated with oxidation–reduction.

INTRODUCTION

Selective catalytic oxidation of methane to syngas (SCO) at short contact times is a promising replacement for the power-consuming process of methane steam reforming [1, 2]. The known catalysts for SCO are metals (nickel and noble metals) supported on oxides. Two main mechanisms of SCO are discussed in the literature. One assumes the total oxidation of methane with further steam or dry reforming of CH_4. The other is a "direct" mechanism, in which methane initially dissociates with the formation of adsorbed hydrogen and methyl radicals (carbon), and then H_2 desorbs, and carbon species are oxidized to CO.

$$CH_4 + \square \longrightarrow CH_{x,\,ads} + (4 - x)H_{ads}, \quad \text{(I)}$$

$$CH_{x,\,ads} \longrightarrow C_{ads} + xH_{ads}, \quad \text{(II)}$$

$$O_{2(gas)} + \square \longrightarrow 2O_{ads}, \quad \text{(III)}$$

$$C_{ads} + O_{ads} \longrightarrow CO, \quad \text{(IV)}$$

$$2H_{ads} \longrightarrow H_2. \quad \text{(V)}$$

Thus, according to this mechanism, the primary products of the reaction are H_2 and CO.

Because the reaction heat of total oxidation of methane is substantial, the first pathway leads to the formation of hot spots and a substantial temperature gradient along the catalyst bed. To exclude these disadvantages, especially when the process is carried out at millisecond contact times, catalysts are necessary that provide the high rate of methane conversion to hydrogen and CO via the second pathway, which is exothermic but with low heat effect (the reaction heat is 8.5 kcal/mol). The rate of transformation is determined by the process of methane dissociation on metallic particles and by the rate of CH_x species interaction with oxygen, whose reactivity depends on the nature of the oxide support [3, 4].

Recent publications reported a high efficiency of the Ce–Zr solid solutions with supported platinum and nickel in both direct oxidation of methane using lattice oxygen without oxygen in the gas phase [5, 6] and in the reactions of steam reforming and selective oxidation of methane by oxygen [7–9]. Our studies of the catalysts for SCO based on Ce–Zr solid solutions supported on corundum monoliths and promoted with small additives of Pt and Rh [10] showed the high activity, selectivity, thermal stability, and resistance to coking in the mixtures with a high concentration of methane (and with possible admixtures of higher hydrocarbons). The use of perovskites $LaNi(Co, Mn)O_3$ promoted with small additives of noble metals (Ni, Pt, Rh, and Ir) as catalyst precursors enables an increase in the activity, selectivity, and resistance to coking [11]. The activity of these catalysts in the form of honeycomb monoliths was determined in the autothermal regime in the reaction mixture with a high concentration of reactants. At the same time, for the development of highly efficient catalysts for SCO that enable the direct pathway of methane conversion into syngas, kinetic data are necessary that are obtained in the presence of oxygen in the gas phase and under conditions that are as close as possible to real conditions, that is, at high temperatures (900–1000°C) and millisecond contact times.

0023-1584/04/4504-0589 © 2004 MAIK "Nauka/Interperiodica"

Table 1. Catalyst chracteristics

Catalyst	Chemical composition of the active component	Phase composition*	Lattice parameters, Å		Particle size, Å
			a	*c*	
ZC-A	$Zr_{0.8}Ce_{0.2}$	$Zr_{0.8}Ce_{0.2}O_2$ SSCS	5.182	–	125
P-ZCA	0.4%Pt/$Zr_{0.8}Ce_{0.2}$	SSCS	5.179	–	105
		Pt			250
N-ZCA	1.3%Ni/$Zr_{0.8}Ce_{0.2}$	SSCS	5.179	–	110
		NiO			50
LN-A	$LaNiO_3$	$LaNiO_3$	5.366	6.579	220
		NiO(traces)			
LN-ZCA	$LaNiO_3$/$Zr_{0.8}Ce_{0.2}$	SSCS	5.182	–	120
		$LaNiO_3$	5.371	6.592	170
		NiO(traces)			
LNP-A	0.2%Pt + $LaNiO_3$	$LaNiO_3$	5.382	6.629	175
LNP-ZCA	0.2%Pt + $LaNiO_3$/$Zr_{0.8}Ce_{0.2}$	SSCS	5.188	–	90
		$LaNiO_3$	5.383	6.625	100
		NiO(traces)			

* Solid solution of the cubic structure.

In this work we studied the SCO activity of Ni, Pt, and lanthanum nickelate (both pure and promoted with Pt) supported on corundum with and without a CeO_2–ZrO_2 sublayer. To maintain the kinetic regime at 900°C and a contact time of ~2 ms, experiments were carried out using a dilute mixture and catalysts with ~100-μm grains. The catalysts were characterized by XRD and temperature-programmed reduction with hydrogen.

EXPERIMENTAL

α-Al_2O_3 with spherical particles (<100 μm) was used as a catalyst support. The specific surface area of the support was 16 m^2/g. According to XRD data, it contains an admixture of θ-Al_2O_3 in a small amount. Catalysts (Table 1) were prepared by incipient-wetness impregnation of Al_2O_3 by the corresponding salt solution. To support the oxide layer $Ce_{0.2}Zr_{0.8}O_2$, the support was impregnated with a solution containing $Ce(NO_3)_3$ and $ZrOCl_2$ in the stoichiometric ratio. Then, samples were dried and calcined in air for 2 h at 900°C. The active components (Ni, $LaNiO_3$, and Pt) were supported from the solutions of $Ni(NO_3)_2$, $La(NO_3)_3$, H_2PtCl_6. The resulting samples were additionally dried and calcined in air for 1 h at 900°C.

XRD analysis of the samples was carried out using a HZG-4C diffractometer (CuK_α irradiation). The average size of particles was determined from the width of the corresponding reflexes using the Sherer equation. Lattice parameters and the size of $LaNiO_3$ particles was estimated from the reflexes with d = 1.9065 and 1.7027 Å corresponding to the (202) and (211) planes (no. 34–1181, JCPDS–ICDD). For the Ce–Zr oxide, these characteristics were determined from the reflexes with d = 1.83094 Å corresponding to the planes (202) of the solid solution CeO_2–ZrO_2.

Temperature-programmed reduction (TPR) by hydrogen was carried out in a flow reactor. Before TPR, samples were calcined in a flow of oxygen at 500°C for 30 min and cooled to room temperature. Then, the flow of oxygen was continuously replaced by a flow of argon and a mixture containing 10 vol % H_2 in Ar. The feed rate was 40 ml/min. The heating ramp from room temperature to 900°C was 10°C/min. In the course of experiments, water was frozen at –80°C. The concentration of hydrogen was determined using a thermal conductivity detector.

The activity of the catalyst was determined at an atmospheric pressure in a flow-type quartz reactor with an inner diameter of 10 mm. The catalyst sample (0.01 g) diluted with quartz powder (0.25–0.5 mm) was fixed inside the reactor between two disks of porous quartz. Temperature was measured using a thermocouple mounted outside of the reactor at the level of the catalyst bed. Before a run, samples were oxidized or reduced. To oxidize a catalyst, it was calcined at 700°C in a flow of oxygen for 1 h and then the temperature was increased to achieve the reaction temperature (900°C). To obtain reduced samples, oxidized catalysts were calcined at 900°C in a flow of a hydrogen–helium mixture for 1 h. Immediately after oxidation or reduction, the reaction mixture 1% CH_4 + 0.5% O_2 in helium was supplied at a rate of 300 ml/min (the contact time was 0.002 s). Before entering the reactor, the reaction mixture passed through a trap at liquid nitrogen temperature. The first analysis of the reaction products was car-

ried out 60 s after the feed was supplied. Samples for analyses were automatically withdrawn every 200 s. The initial mixture and reaction products were analyzed using a Tsvet-500 chromatograph. The conversion of methane and selectivity for the products were calculated from the carbon balance.

RESULTS

Phase Composition and the Size of Particles

Some characteristics of the catalysts and their compositions are shown in Table 1. According to XRD data, supported cerium and zirconium oxides form a solid solution with a cubic structure. The lattice parameter of the solid solution changes insignificantly for all the samples and is close to 5.182 Å, whereas the average size of particles (the region of coherent scattering) decreases when the active component (especially Pt-containing) is supported. In the samples with supported lanthanum nickelate, both pure and promoted with platinum, the hexagonal perovskite phase dominates. On the XRD patterns of the samples LN-A, LNP-A, and LNP-ZCA, there are broad lines corresponding to NiO and pointing to the presence of highly dispersed nickel oxide particles. At the same time, for Pt-containing catalysts, platinum reflexes were not observed. This can be due to the low concentration of Pt and to the incorporation of metal cations in the perovskite structure.

For lanthanum nickelate supported on pure corundum (sample LN-A), a noticeable decrease in the lattice parameter a takes place (Table 1) compared to the bulk perovskite ($a = 5.451$, $c = 6.564$; no. 34–1181, JCPDS-ICDD), whereas the parameter b changes insignificantly. This points to the distortion of the structure of supported perovskite, possibly due to the epitaxial interaction with the support as it was observed by us in [12]. Note that unlike papers [12, 13] where supported lanthanum nickelate had a cubic structure, here we observed the hexagonal phase of perovskite, which is typical of the nonstoichiometric $LaNiO_{3-x}$ [18]. The difference in the structures of perovskite depending on the oxygen stoichiometry can be due to the effect of support: in previous studies, pure corundum with a surface area of ~5 m^2/g was used, whereas here the support had a surface area of 16 m^2/g and contained a θ-Al_2O_3 admixture. The addition of platinum (sample LNP-A) led to an increase in the lattice parameters and to a decrease in the average sizes of perovskite structures.

For the LN-ZCA sample based on corundum with the Ce–Zr oxide sublayer, an increase in the lattice parameters of supported lanthanum nickelate compared to the LN-A sample is observed. Thus, the presence of the oxide sublayer, as well as the addition of Pt, leads to the distortion of the perovskite structure. At the same time, for lanthanum nickelate promoted by platinum, the value of lattice parameters is practically independent of the presence of oxide support: the structural characteristics of perovskite in the samples LNP-ZCA and LNP-A are practically the same (Table 1). The use of oxide support is favorable for an increase in the dispersity of perovskite, both pure (LN-ZCA) and promoted with platinum (LNP-ZCA).

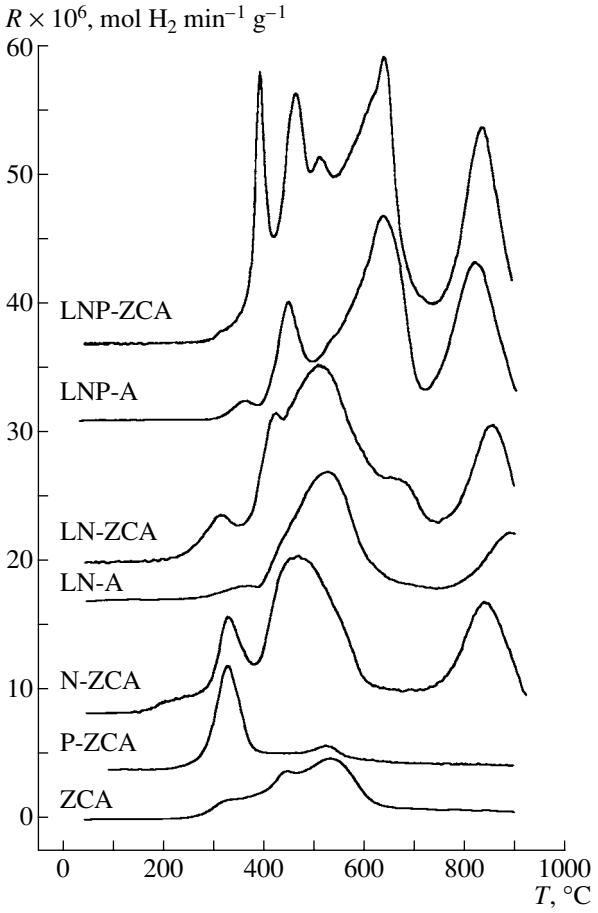

Fig. 1. Dependence of the rate of hydrogen consumption on temperature in temperature-programmed reduction by hydrogen.

TPR by Hydrogen

TPR curves for the studied samples are shown in Fig. 1. It is known that the addition of zirconium to ceric oxide leads to a significant shift of the maximum of reduction of solid solution toward the low-temperature region [14]. This points to the presence of the reactive bulk oxygen bound to defects in the structure of bulk solid solutions $Ce_xZr_{1-x}O_2$ [6]. For supported $Ce_{0.2}Zr_{0.8}O_2$ (sample ZCA), we observed three maxima of the rate of hydrogen consumption at 312, 440, and 530°C, which points to the high reactivity of both surface and lattice oxygen. The addition of platinum practically does not affect the overall amount of removed oxygen but significantly increases the amount of oxygen removed at low temperatures. This is evident from the presence of an intense maximum at 325°C in the spectrum of the P-ZCA sample. A decrease in the tem-

Table 2. Characteristics of catalyst activity in the selective oxidation of methane: oxidized samples

Catalyst	Conversion, %				Selectivity for CO, %		H_2/CO		Induction period, min
	CH_4		O_2						
	1	*2*	*1*	*2*	*1*	*2*	*1*	*2*	
LN-A	9	5	30	17	27	15	–	–	–
LNP-A	14 (34)	28	59 (88)	77	3 (94)	69	– (5)	0.9	11.5
ZCA	17	15	58	57	12	8	–	–	–
P-ZCA	22	23	89	91	25	15	–	–	–
N-ZCA	66	38	93	87	95	84	2.1	1.44	–
LN-ZCA	50	35	94	74	95	74	1.4	1	–
LNP-ZCA	5 (39)	20	28 (86)	81	10 (79)	33	– (1.4)	0.5	105

Note: (*1*) Initial value; (*2*) after 6.5 h. The maximal values achieved after the induction period are given in parentheses.

perature of reduction of solid solutions CeO_2–ZrO_2 in the presence of platinum is explained by the known effect of hydrogen atom spillover onto the oxide [15]. Hydrogen atoms are formed by the dissociative adsorption of hydrogen on noble metals.

For N-ZCA we observed three maximums of the rate at 330, 470, and 840°C. An increase in the overall amount of oxygen removed corresponds to the reduction of NiO. Supported nickel, as well as platinum, favors hydrogen spillover and facilitates the reduction of solid solutions CeO_2–ZrO_2. The low-temperature maximum, which is close in its intensity and position to the maximum in the analogous sample containing platinum, can largely be explained (in agreement with data [16]) by the removal of oxygen of the solid solution. However, highly reactive oxygen of separate nickel oxide clusters can make a small contribution to this peak [7], although complete reduction of corundum-supported nickel oxide takes place at a higher temperature [17]. An intense maximum at 470°C corresponds to the respective position of maximum for NiO [17], which assumes the presence of nickel oxide in the catalyst, whose oxygen is about equally reactive as oxygen in the bulk oxide. The appearance of the high-temperature maximum can be associated with the penetration of nickel cations to the subsurface layer of oxide support and with their harder reduction.

The reduction of corundum-supported lanthanum nickelate occurs at higher temperatures than in the case of bulk $LaNiO_3$ [18]. In the spectrum of $LaNiO_3$ supported on pure corundum (LN-A), the following maximums are observed: a small maximum at ~350°C, the high-intensity maximum at 530°C, and the incompletely resolved one at 890°C. We assume that, by analogy with the stoichiometric $LaNiO_3$, maximums at 350 and 530°C correspond to the removal of the most reactive oxygen from perovskite, whereas the high-temperature maximum corresponds to the complete perovskite reduction to Ni and La_2O_3 [18]. This is supported by the fact that the phase composition of LN-A reduced at 500°C corresponds to the initial perovskite. More difficult reduction of supported $LaNiO_3$ is due to its interaction with the support, which is evident from the lattice parameters divergence from the parameters of bulk perovskite (Table 1). For lanthanum nickelate supported on corundum with the oxide support (LN-ZCA), we observed a shift of peaks toward the low-temperature region. In addition to that, unresolved maximums at 420 and 670°C appear. Thus, in the presence of the $Ce_{0.2}Zr_{0.8}O_2$ support, the removal of oxygen from $LaNiO_3$ takes place. We believe that this is due to different degrees of disorder in the structure of perovskite supported on corundum and the $Ce_{0.2}Zr_{0.8}O_2$ sublayer, which is evident from an increase in the lattice parameter *c* for $LaNiO_3$.

The addition of platinum strongly affects the dependence of the rate of hydrogen consumption by $LaNiO_3$ supported on pure corundum (LNP-A) and corundum with the oxide sublayer (LNP-ZCA). For LNP-A, the low-temperature maximum at ~350°C is more pronounced and intense maximums at 450 and 650°C appear. The high-temperature maximum is shifted by 70°C toward lower temperatures compared to the dependence for the LN-A sample. Thus, we assume that due to the spillover effect, the addition of platinum leads to the removal of a larger amount of reactive oxygen from perovskite at low temperatures and to a decrease in the temperature of its complete reduction. Dependence of the rate of hydrogen consumption for LNP-ZCA is more complex compared to LNP-A: at a temperature lower than 550°C, three maximums are observed, and the position of maximums at temperatures above 600°C changes insignificantly. A complex form of this dependence points to the presence of various forms of oxygen, which is due to the complex composition of the catalyst.

Catalytic Activity

Oxidized catalysts. In Table 2 the values of initial conversion (after 60 s) and conversions after 6.5 h for

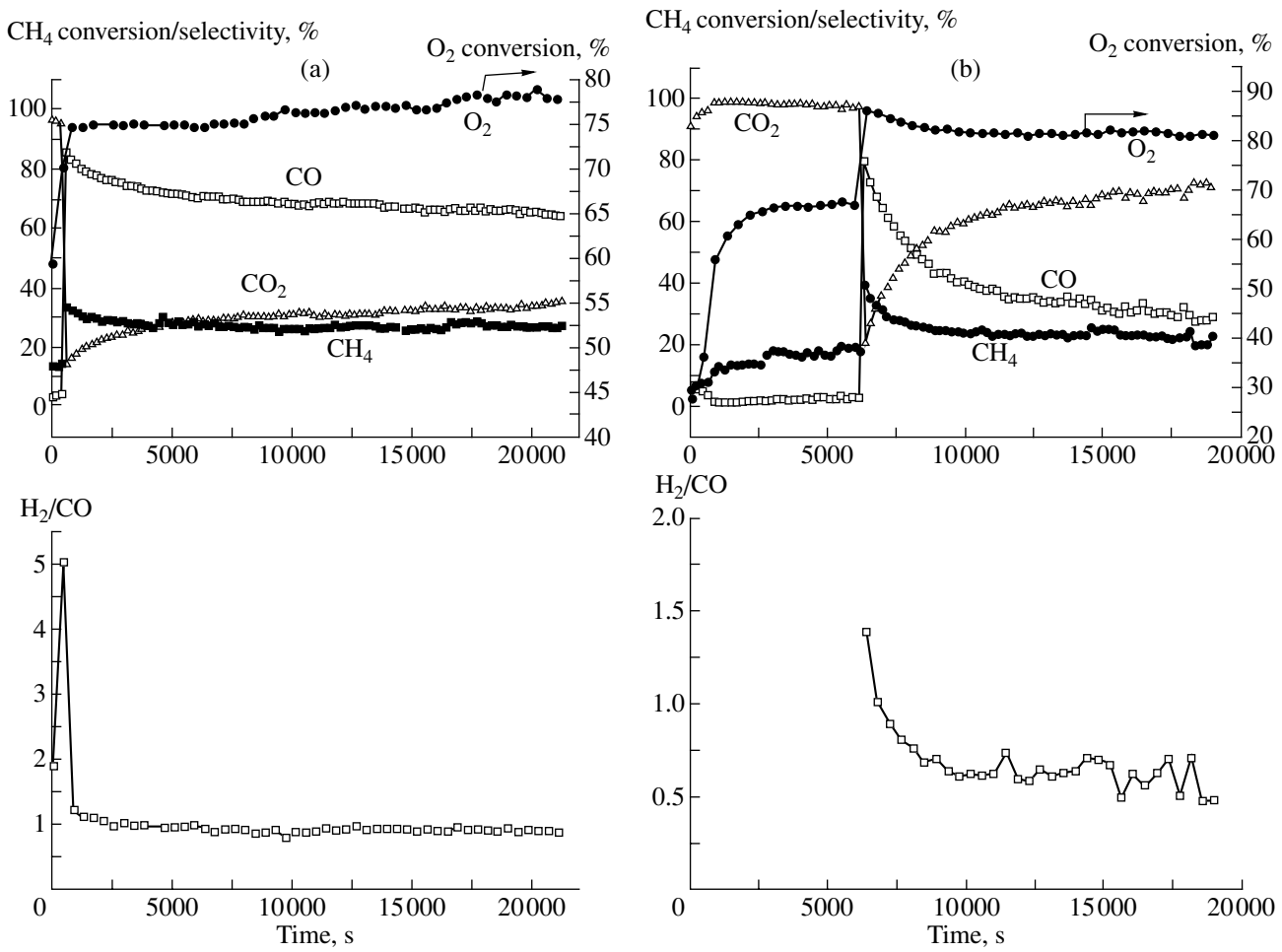

Fig. 2. Dependence of the methane and oxygen conversion, the selectivity for the reaction product, the H_2/CO ratio on the reaction time for the oxidized samples (a) LNP-A and (b) LNP-ZCA.

methane and oxygen, the selectivities to CO, and the H_2/CO ratio for the oxidized samples are presented. Supported $Ce_{0.2}Zr_{0.8}O_2$ (ZCA) has a low activity and selectivity for syngas in the presence of oxygen in the gas phase. The addition of platinum (P-ZCA) leads to a slight increase in the conversion and selectivity for CO.

The sample N-ZCA containing nickel has the highest activity, and the initial values of conversion and selectivity for syngas are maximal, followed by a slow decrease. Simultaneously, the H_2/CO ratio also decreases. The level of activity of LN-ZCA containing lanthanum nickelate is somewhat lower, but the nature of its change is the same as for N-ZCA, except for the lower value of H_2/CO. Note that the activity of $LaNiO_3$ supported on pure corundum (LN-A) is low.

The addition of platinum to the sample based on $LaNiO_3$ leads to the appearance of an induction period; this period is longer for the LNP-ZCA sample (Fig. 2). During the induction period, low conversions of methane and oxygen and a low selectivity for syngas are observed, then gradually these characteristics start to increase. A further change in the selectivity for syngas is determined by the presence of an oxide sublayer: the selectivity for CO of the sample LNP-A (Fig. 2a) slowly decreases, but it remains much higher than the selectivity for CO_2, whereas for the sample LNP-ZCA (Fig. 2b), the selectivity for CO rapidly decreases, and after ~40 min CO_2 becomes the main reaction product. The value and the nature of changes in the H_2/CO ratio for the samples LNP-A and LNP-ZCA are substantially different, which points to the difference in the pathways of methane conversion on these samples.

Reduced samples. Table 3 shows data on the activity of reduced samples. For the reduced sample ZCA, we observed an increase in the conversion of methane and oxygen compared to the oxidized sample, and the selectivity for syngas remains low. The addition of platinum leads (as in the case of the oxidized sample) to some growth in the conversion and selectivity, but the main product is CO_2.

The initial selectivity for syngas for the reduced sample N-ZCA is close to 100%, and the conversion of methane is 20% lower than in the case of the oxidized sample. A fast decrease in the activity and selectivity

Table 3. Characteristics of the catalyst activity in the selective catalytic oxidation of methane: reduced sample

Catalyst	Conversion, %				Selectivity for CO, %		H_2/CO		Induction period, min
	CH_4		O_2						
	1	*2*	*1*	*2*	*1*	*2*	*1*	*2*	
LN-A	8	4	20	10	30	31	–	–	
LNP-A	25 (70)	48	97	99	5 (94)	78	– (6)	1.94	18.5
ZCA	23	20	82	76	10	9	–	–	–
P-ZCA	26	30	96	96	19	24	–	–	–
N-ZCA	45	15	96	55	99	7	1	–	–
LN-ZCA	19 (78)	65	66 (99)	99	4 (96)	97	– (2.7)	2.1	58
LNP-ZCA	27 (65)	31	96	97	5 (87)	36	– (2)	0.9	40

Note: (*1*) Initial value; (*2*) after 6.5 h. The maximal values achieved after the induction period are given in parentheses.

with time is observed, and ~100 min after the reaction mixture is admitted to the reactor, CO_2 dominates in the reaction products (Fig. 3). For the reduced samples containing lanthanum nickelate (except for LN-A whose activity is very low), an induction period is observed, the value of which depends on the composition of the catalysts (Table 3, Figs. 4, 5). LNP-A (Fig. 5a) has a shorter induction period, as in the case of oxidized samples (Table 2). The induction periods for the samples LN-ZCA and LNP-ZCA are 58 and 40 min, respectively. A change in the methane conversion and selectivity for syngas for these preliminarily reduced catalysts has the same character as for the oxidized samples (Figs. 4, 5). At the same time, in the case of reduced samples containing platinum, the high initial conversion of oxygen is preserved in the course of the reaction. The highest conversion and selectivity for syngas are achieved in the case of LNP-A (Fig. 5a) and LN-ZCA (Fig. 4). For the first of these samples, the selectivity decreases with time, whereas the selectivity of LN-ZCA remains constant in the course of experiments. Note also that for these samples, the H_2/CO ratio is ~2 and does not change with time.

Changes in the conversion of methane and oxygen and the selectivity for syngas for the catalyst LNP-ZCA are shown in Fig. 5b. As in the case of the oxidized sample (Fig. 2b), the reduced LNP-ZCA sample shows a rather fast decrease in the conversion and selectivity for syngas. An interesting feature of this catalyst is the oscillating selectivity.

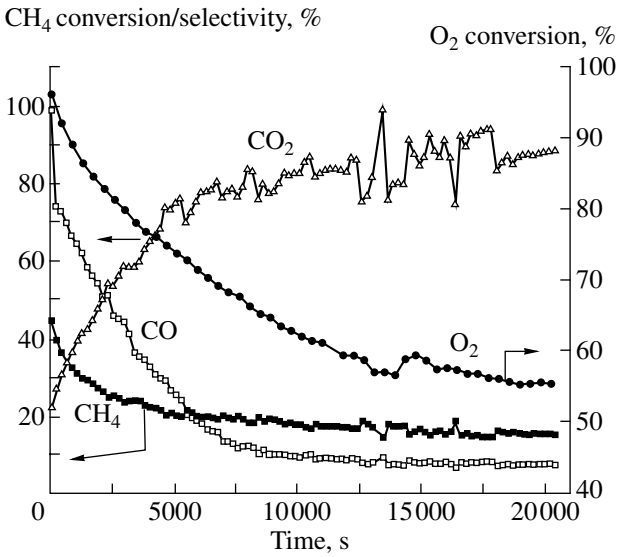

Fig. 3. Dependence of the methane and oxygen conversion, the selectivity for the reaction products on the reaction time for the reduced N-ZCA sample.

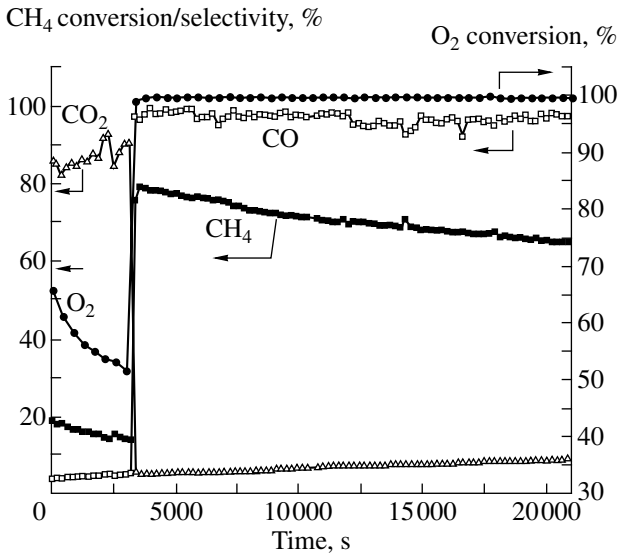

Fig. 4. Dependence of the methane and oxygen conversion, the selectivity for the reaction products on the reaction time for the reduced LN-ZCA sample.

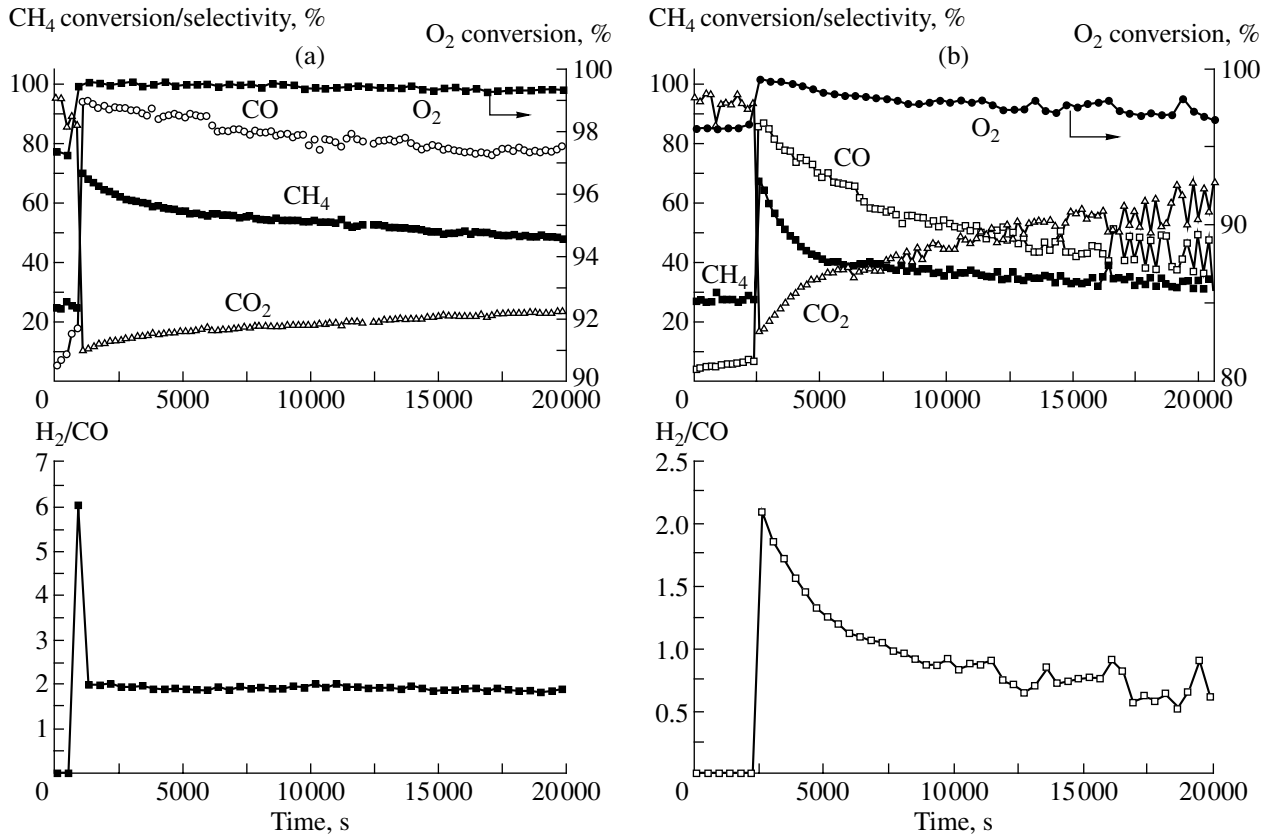

Fig. 5. Dependence of the methane and oxygen conversion, the selectivity for the reaction products, and the H_2/CO ratio on the reaction time for the reduced samples (a) LNP-A and (b) LNP-ZCA.

DISCUSSION

The results obtained suggest that the behavior of catalysts studied in SCO is determined not only by preliminary treatment but also by the chemical composition.

It was shown in [19, 20] that different states of the Ni/Al_2O_3 surface correspond to different pathways of SCO. On the completely oxidized catalyst, total oxidation of methane to water and CO_2 takes place. The conversion of reactants and the selectivity for syngas are low. For SCO the reduction of NiO is necessary because the dissociative activation of methane only takes place on reduced Ni^0 sites.

It is assumed that, in the case of Ni/Al_2O_3, the activation of both methane and oxygen occurs on Ni^0 with the formation of surface intermediates Ni…C and $Ni^{\delta+}…O^{\delta-}$. Due to their interaction, CO is formed as a primary product. In the case of the $Ni/(CeZr)O_2$ catalysts, the activation of oxygen may occur with the participation of support [9]. Solid solutions $Ce_xZr_{1-x}O_2$ are a source of highly mobile oxygen, which is capable of oxidizing carbon formed on metallic Ni particles or preventing its formation via oxygen spillover onto Ni particles [5–7].

The initial activity of oxidized samples and the dynamics of the reaction are determined by the formation of Ni^0 particles during contact of the oxidized catalyst surface with the reaction mixture. The maximal initial values of methane and oxygen conversions and the selectivity for syngas in the case of N-ZCA and LN-ZCA sample (Table 2) point to the fast reduction of nickel to form Ni^0 particles. Taking into account experimental conditions (900°C and a contact time of ~0.002 s), we assume that the high selectivity for syngas for these samples is due to the occurrence of the reaction via the direct pathway (reactions (I)–(V)) involving the interaction of a carbon species formed in CH_4 dissociation with an adsorbed oxygen species with the formation of CO. Note also that the high activity and selectivity of these samples can be due to the high dispersity and defectness of Ni^0 particles under the action of reaction medium [20].

In the case of LN-ZCA, the lower value of the H_2/CO ratio at ~100% carbon balance is likely to be due to the higher rate of hydrogen oxidation. However, we cannot exclude some contribution from the pathway and the products of total oxidation. It is known that the presence of lanthanum oxides and zirconia in the catalysts is favorable for the activation of CO_2 and, corre-

spondingly, favors the occurrence of methane dry reforming [21].

Preliminary reduction of samples at 900°C in hydrogen radically changes the activity of almost all samples (Table 2). Thus, for the reduced N-ZCA sample (Fig. 3), at a high initial selectivity for syngas, the conversion of methane is lower than for the oxidized sample, and the activity rapidly decreases. The lower conversion of methane could be due to the lower dispersity of metallic nickel after high-temperature reduction in hydrogen and the absence of surface defects. A drastic decrease in activity is primarily due to metallic particle oxidation to NiO. One can assume that the oxidation of metallic nickel occurs as a result of diffusion or spillover of active mobile oxygen, which is generated on the reduced sites of the oxide Ce–Zr support to the surface of the metal [22]. At the same time, the reduced LN-ZCA sample has a high activity and stability (Fig. 4). In this case, lanthanum oxide formed by the reduction of supported $LaNiO_3$ can be a buffer between the particles of reduced nickel and Ce–ZrO_2 and can thus prevent metal oxidation.

When platinum is added, the activity of supported $LaNiO_3$ depends on the presence of an oxide sublayer in the catalyst: for LNP-ZCA, the conversion of methane and the selectivity for syngas are lower than those of the LN-ZCA and LNP-A samples (Table 2). We may assume that the presence of both platinum and Ce–ZrO_2 in the catalyst is favorable for the activation of oxygen adsorbed from the gas phase and lattice oxygen of oxide support. As a result, the main pathway of the reaction becomes the total oxidation of methane with the formation of CO_2 and water.

The induction period is observed for both oxidized and reduced samples LNP-A and LNP-ZCA (Figs. 2 and 5) and for the reduced sample LN-ZCA not promoted with platinum (Fig. 4). It is well known that long relaxations cannot be due to a simple change in the oxidation state of the surface. They usually reveal themselves when other processes occur, such as a change of phase, diffusional exchange of surface active sites with a high buffer volume (crystallite bulk), or restructuring induced by a change in the stoichiometry of the sample. For the cerium–zirconium oxide solid solutions, the high mobility of the lattice oxygen, which increases when platinum is introduced into the near-surface layer [6], as well as a high buffer capacity, may be favorable for the appearance of long relaxations when either a reduced or an oxidized sample is used initially. Another important factor can be the accumulation of carbonate complexes on the surface and/or its hydroxylation. This factor is most likely to reveal itself in the case of samples containing lanthanum compounds in the surface layer, because lanthanum hydroxocarbonates are much more thermally stable than cerium and zirconium hydroxocarbonates. Because hydroxocarbonates usually block surface sites responsible for the activation of molecular oxygen, one may expect that their accumulation will favor a decrease in the selectivity for the total oxidation products. The high (>2) values of the H_2/CO ratio at the moment of catalyst activation suggest that carbonates and/or carbon are accumulated on the catalyst surface during the induction period (Figs. 2, 5)

We may assume that, in the case of oxidized samples, the induction period is largely due to the dynamics of phase reduction of lanthanum nickelate to Ni^0 coupled with the formation of a partially hydrated and carbonized surface layer. In the case of reduced samples where metallic nickel is present from the start, the induction period clearly has a more complex nature. It is known that oxygen adsorption on the pure surface of metallic nickel is very fast and the sticking coefficient of oxygen is ~1 [23]. We may assume that, when the reaction mixture is supplied to the freshly reduced catalyst, oxygen is mostly adsorbed and the oxidation of the near-surface layer of nickel particles takes place because of the strong difference in the rates of adsorption of methane and oxygen. This means that for the reduced samples, slow relaxations cannot be due to a change in the oxidation state of nickel particles. At the same time, the oxidation of reduced cerium–zirconium oxide solid solution, which is accompanied by a change in its defect structure [6] and carbonization of the surface layer, is rather slow [24]. This helps to understand why long relaxations are also observed for the reduced samples. A shorter induction period for the reduced sample LNP-A (Fig. 5a) compared to LNP-CZA, containing cerium–zirconium solid solution (Fig. 5b), may indicate a certain relation between slow relaxations and processes that change its composition and structure under the action of the reaction medium. Obviously, a more detailed explanation for long relaxations will only be possible if *in situ* studies of the catalyst state in the reaction medium are carried out because side processes are very complex.

REFERENCES

1. Tsang, S.C., Claridge, J.B., and Green, M.L., *Catal. Today*, 1995, vol. 23, p. 3.
2. Arutyunov, V.S. and Krylov, O.V., *Okislitel'nye prevrashcheniya metana* (Oxidative Conversions of Methane), Moscow: Nauka, 1998, p. 362.
3. Slaa, J.C., Berger, R.J., and Marin, G.B., *Catal. Lett.*, 1997, vol. 43, p. 63.
4. Wang, H.Y. and Ruckenstein, E., *J. Phys. Chem. B*, 1999, vol. 103, p. 11327.
5. Otsuka, K., Wang, Y., and Nakamura, M., *Appl. Catal., A*, 1999, vol. 183, p. 317.
6. Sadykov, V.A., Kuznetsova, T.G., *et al.*, *React. Kinet. Catal. Lett.*, 2002, vol. 76, p. 83.
7. Dong, W.-S., Roh, H.-S., Jun, K.-W., Park, S.-E., and Oh, Y.-S., *Appl. Catal., A* 2002, vol. 226, p. 63.
8. Shishido, T., Sukenobu, M., *et al.*, *Appl. Catal., A*, 2002, vol. 223, p. 35.
9. Roh, H.-S., Dong, W.-S., Jun, K.-W., and Park, S.-E., *Chem. Lett.*, 2001, p. 88.

10. Pavlova, S.N., Sadykov, V.A., Parmon, V.N., Bobrova, I.I., Zolotarskii, I.A., Kuzmin, V.A., Salanov, A.N., Bunina, R.V., Saputina, N.F., Snegurenko, O.I., and Vostrikov, Z.Yu., *EUROPACAT-V, A Book of Abstracts*, 2001, vol. 4, p. 5-0-04.
11. Sadykov, V.A., Paukshtis, E.A., Burgina, E.B., Degtyarev, S.P., Kochudei, D.I., Kalinkin, A.V., Saputina, N.F., Roy, R., and Agrawal, D., *Stud. Surf. Sci. Catal.*, 1998, vol. 119, p. 759.
12. Pavlova, S.N., Sadykov, V.A., Saputina, N.F., Zaikovskii, V.I., Kalinkin, A.V., Kustova, G.N., Tsybulya, S.V., Zolotarskii, I.A., Bunina, R.V., and Tikhov, S.F., *CHISA-98 Summaries*, 1998, vol. 2, P7.24, p. 72.
13. Isupova, L.I., Alikina, G.A., *et al.*, *Catal. Today*, 2002, vol. 75, p. 305.
14. Vidal, H., Kaspar, J., Pijolat, M., Colon, G., Bernal, S., Cordon, A., Perrichon, V., and Fally, F., *Appl. Catal., B*, 2001, vol. 30, p. 75.
15. Fornasiero, P., Kaspar, J., Sergo, V., and Graziani, M., *J. Catal.*, 1999, vol. 182, p. 56.
16. Takeguchi, T., Furukawa, S., and Inoue, M., *J. Catal.*, vol. 202, p. 14.
17. Cao, L., Chen, Y., and Li, W., *Stud. Surf. Sci. Catal.*, 1997, vol. 107, p. 467.
18. Rakshit, S. and Gopalakrishnan, P.S., *J. Solid. Stat. Chem.*, 1994, vol. 110, p. 28.
19. Li, C., Yu, C., and Shen, S., *Catal. Lett.*, 2000, vol. 67, p. 139.
20. Jin, R., Chen, Y., Cui, W., Ji, Y., Yu, C., and Jiang, Y., *Appl. Catal., A*, 2000, vol. 201, p. 71.
21. Bradford, M.C.J. and Vannice, M.A., *Catal. Rev.–Sci. Eng.,* 1999, vol. 41, no. 1, p. 1.
22. Fathi, M., Bjorgum, E., Viig, T., and Rokstad, O.A., *Catal. Today*, 2000, vol. 63, p. 489.
23. Dadayan, K.A., Boreskov, G.K., Savchenko, V.I., and Bulgakov, N.N., *Kinet. Katal.*, 1977, vol. 18, no. 3, p. 574.
24. Roh, H.-S., Jun, K.-W., Baek, S.-C., and Park, S.-E., *Chem. Lett.*, 2001, p. 1048.